Calorimetric studies on the stability of the ribosome-inactivating protein abrin II: effects of pH and ligand binding

Jayarapu KRUPAKAR*, Chittoor P. SWAMINATHAN†, Puspendu K. DAS*, Avadhesha SUROLIA†[1] and Sunil K. PODDER‡

*Department of Inorganic and Physical Chemistry, Indian Institute of Science, Bangalore-560 012, India, †Molecular Biophysics Unit, Indian Institute of Science, Bangalore-560 012, India, and ‡Department of Biochemistry, Indian Institute of Science, Bangalore-560 012, India

The effects of pH and ligand binding on the stability of abrin II, a heterodimeric ribosome-inactivating protein, and its subunits have been studied using high-sensitivity differential scanning calorimetry. At pH 7.2, the calorimetric scan consists of two transitions, which correspond to the B-subunit [transition temperature (T_m) 319.2 K] and the A-subunit (T_m 324.6 K) of abrin II, as also confirmed by studies on the isolated A-subunit. The calorimetric enthalpy of the isolated A-subunit of abrin II is similar to that of the higher-temperature transition. However, its T_m is 2.4 K lower than that of the higher-temperature peak of intact abrin II. This indicates that there is some interaction between the two subunits. Abrin II displays increased stability as the pH is decreased to 4.5. Lactose increases the T_m values as well as the enthalpies of both transitions. This effect is more pronounced at pH 7.2 than at pH 4.5. This suggests that ligand binding stabilizes the native conformation of abrin II. Analysis of the B-subunit transition temperature as a function of lactose concentration suggests that two lactose molecules bind to one molecule of abrin II at pH 7.2. The presence of two binding sites for lactose on the abrin II molecule is also indicated by isothermal titration calorimetry. Plotting ΔH_m (the molar transition enthalpy at T_m) against T_m yielded values for ΔC_p (change in excess heat capacity) of 27 ± 2 kJ·mol^{-1}·K^{-1} for the B-subunit and 20 ± 1 kJ·mol^{-1}·K^{-1} for the A-subunit. These values have been used to calculate the thermal stability of abrin II and to surmise the mechanism of its transmembrane translocation.

Key words: differential scanning calorimetry, isothermal titration calorimetry, lactose binding, protein stability, thermal denaturation.

INTRODUCTION

Abrin II, a type II ribosome-inactivating protein (RIP) from *Abrus precatorius* seeds, consists of two subunits, the A-subunit (M_r 30000) and the B-subunit (M_r 33000), which are connected via a single disulphide bond [1]. The A-subunit is an N-glycosidase, and inactivates eukaryotic protein synthesis by cleaving the base adenine-4324 from the 28 S rRNA [2]. The B-subunit is a lectin, which binds to the cell-surface receptor that contains terminal galactose residues, thus facilitating the entry of the toxic A-subunit into the cell [3–6]. Reduction of the inter-subunit disulphide bond is necessary for the toxin to initiate its action [7]. The late endosomes and Golgi apparatus are implicated for the transmembrane transfer of the toxic A-subunit to the cytosol [8,9]. Recently it has been argued that the endoplasmic reticulum is the probable site of such a translocation [10,11]. Although the mechanism underlying the transmembrane transport of RIPs is not fully understood, these proteins have been used extensively for the construction of immunotoxins for therapeutic purposes. and have been useful as models for studies of the mechanisms by which soluble proteins are able to cross the membrane.

With regard to the action of toxins, the process of cell intoxication by diphtheria toxin (DT) is best understood. Subsequent to endocytosis, the endosomal pH induces conformational changes in DT, resulting in the transport of its A-subunit into the cytosol through the endosomal membrane [12]. *In vitro*, at low pH, DT undergoes partial unfolding. As a result it opens up the buried hydrophobic patches, which enable it to be translocated [13,14]. Abrin II, like DT, is a water-soluble protein, but in order to reach the ribosomes it has to cross the membrane. Earlier studies have shown that, at low pH, ricin (a type II RIP) and its subunits penetrate membranes [15,16]. Abrin II is expected to follow a similar itinerary within the cell.

A detailed thermodynamic study of abrin II will aid in the understanding of the mechanism of its transfer to the cytosol. Unfolding experiments using guanidine hydrochloride have demonstrated that, at low pH, ricin, mistletoe lectin and their A-subunits show an increase in stability, whereas their B-subunits show decreased stability [17,18]. In the present study, we investigate the effects of pH and ligand binding on the stability of abrin II by means of high-sensitivity differential scanning calorimetry (DSC). In these studies DSC has been used to determine the transition temperature (T_m) for the unfolding of abrin II, the calorimetric and van't Hoff enthalpies (ΔH_c and ΔH_v respectively), and the change in excess heat capacity (ΔC_p). Taken together, these data provide information on the conformational stability of the protein.

MATERIALS AND METHODS

Materials

DEAE-Sephacel, Sepharose-4B and Sephadex G-100 used for protein purification were products of Pharmacia (Uppsala, Sweden). Ultrapure lactose and dithiothreitol were obtained from Sigma Chemical Co. (St. Louis, MO, U.S.A.). All other chemicals used were of analytical grade and were obtained locally. Abrin II was isolated from seeds of *Abrus precatorius* using the procedure in [19]. The A-subunit of abrin II was

Abbreviations used: DSC, differential scanning calorimetry; ITC, isothermal titration calorimetry; RIP, ribosome-inactivating protein; DT, diphtheria toxin; C_p, excess heat capacity; ΔC_p, change in excess heat capacity; T_m, transition temperature; T_p, temperature of the peak maximum; ΔH_m, molar transition enthalpy at T_m; ΔH_c calorimetric enthalpy; ΔH_v, van't Hoff enthalpy; n, number of binding sites.

[1] To whom correspondence should be addressed (e-mail surolia@mbu.iisc.ernet.in).

purified as described in [20]. The concentrations of abrin II and of its A-subunit were determined from their respective molar absorption coefficients at 280 nm of 100170 $M^{-1} \cdot cm^{-1}$ and 23610 $M^{-1} \cdot cm^{-1}$ [19,20].

DSC

All calorimetric measurements were carried out with a Microcal MC-2 ultrasensitive differential scanning calorimeter. DSC measurements were carried out as a function of scan rate, pH, and protein and ligand concentrations. The data were analysed using Origin® software supplied by the DSC manufacturer. The ratio $\Delta H_c/\Delta H_v$ was utilized to infer the co-operativity of the transition. ΔH_v is calculated from the equation:

$$\Delta H_v = 4\boldsymbol{R}T_m^2 C_{p(max)}/\Delta H_c \quad (1)$$

where $\boldsymbol{R}$ is the gas constant, $C_{p(max)}$ is the maximal value of the excess heat capacity and T_m is the temperature at $C_{p(max)}$. The binding constant of lactose to the protein at the denaturation temperature $[K_b(T_c)]$ is obtained from the following equation [21,22]:

$$K_b(T_c) = \{\exp[(T_c - T_m)\Delta H_c/n\boldsymbol{R}T_c T_m] - 1\}/[L] \quad (2)$$

where T_c and T_m are the denaturation temperatures in the presence and absence of lactose respectively, ΔH_c is the calorimetric enthalpy of the lactose–protein complex, [L] is the ligand concentration and n is the number of binding sites in the protein.

The protein samples were dialysed extensively with large volumes of the desired buffer and degassed prior to loading into the calorimetric cell. The sample pH was checked both before and after the scan. The buffers used were 50 mM sodium acetate for the pH range 4.5–5.8, 50 mM sodium phosphate for the pH range 6.4–7.9, 50 mM sodium borate for the pH range 8.3–9.2, and 50 mM sodium carbonate for pH 10.16. β-Mercaptoethanol (5 mM) was added to the buffer systems for experiments with the A-subunit of abrin II.

Isothermal titration calorimetry (ITC)

Isothermal calorimetric titrations were performed with an Omega microcalorimeter (Microcal), as described in [23,24]. Defined aliquots (5 μl) of lactose solution (10.5 mM) were added from the computer-controlled 250 μl rotating syringe (395 rev./min) to the protein solution (0.351 mM) kept in a 1.347 ml cell, and heat changes accompanying the additions were recorded. The time period between two consecutive injections was 2.5 min, to allow the exothermic peak, which appeared after each addition, to return to the baseline. The area under each peak represented the amount of heat accompanying binding of the added lactose to the protein. The total heat, Q_t, was then fitted via a non-linear least-squares minimization method to the total lactose concentration, X_t, using the following equation:

$$Q_t = nM_t\Delta H_b V\{1 + X_t/nM_t + 1/nK_bM_t - [(1 + X_t/nM_t + 1/nK_bM_t)^2 - 4X_t/nM_t]^{\frac{1}{2}}\}/2 \quad (3)$$

where n is the number of binding sites, M_t is the total protein concentration, V is the cell volume, K_b is the binding constant and ΔH_b is the binding enthalpy. The heat released for the ith injection, ΔQ_i, is given by the following equation

$$\Delta Q_i = Q_i + dV_i/2V[Q_i + Q_{i-1}] - Q_{i-1} \quad (4)$$

where dV_i is the volume of the titrant added to the protein solution.

RESULTS

Thermal unfolding of abrin II

A plot of the baseline-subtracted excess heat capacity (C_p) against temperature for abrin II in 50 mM sodium phosphate buffer, pH 7.2, at a scan rate of 10 $K \cdot h^{-1}$ is shown in Figure 1 (upper curve). The respective baseline-subtracted data (where the baseline was obtained with buffer in both the sample and the reference cuvettes of the calorimeter) were used for all analyses. The pre- and post-transition baselines were connected by the progress baseline option of the Origin® program and subtracted from the data, as shown in Figure 2. The free energy of unfolding of a protein can be obtained as a function of temperature, in principle, from a single DSC experiment by Gibbs–Helmholtz analysis of the DSC data. In practice, however, it is difficult to determine the ΔC_p of unfolding accurately from a single scan. The measurement of ΔH_c as function of T_m, obtained by carrying out DSC scans at different pH values, allows the estimation of ΔC_p from the slope of a plot of ΔH_c against T_m. The value of ΔC_p obtained by this method is considered a better estimate than that obtained directly as the difference between the pre- and post-transition baselines in a single DSC experiment, because the latter method is fraught with errors due to arbitrariness in baseline determination [25–28].

In the abrin II system, we have found that the ΔH_c against T_m plot is fitted well by a straight line (correlation coefficients are 0.97 and 0.98 for the lower- and higher-temperature transitions respectively) over a range of T_m values. In Figure 1, the dashed and the dotted–dashed lines are the deconvoluted least-squares fits of the calorimetric data to a two-state transition model for each of the two transition peaks. The sum of these two transition peaks is represented by the continuous line, which follows closely the observed curve, represented by open circles. The lower-temperature transition peak has a T_m of 319.2 K with ΔH_m =

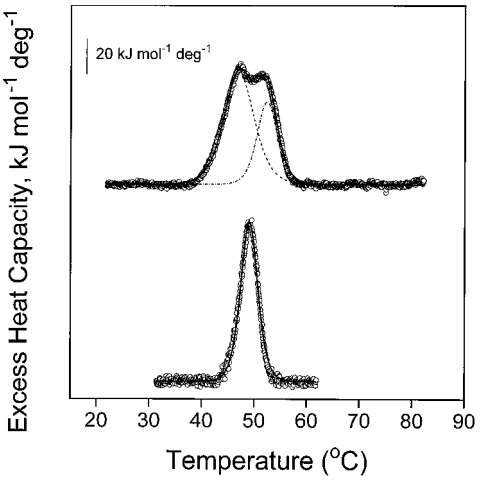

Figure 1 Calorimetric scans of abrin II and its A-subunit

Upper curve: plot of C_p against temperature for abrin II (92.8 μM) at pH 7.2 at a scan rate of 10 $K \cdot h^{-1}$. The progress baseline-subtracted and concentration-normalized DSC data for abrin II are resolved into two independent two-state curves. The data points are shown as open circles (○). The two-state fits of the data to lower- and higher-temperature transitions are shown as a dashed line and a dotted–dashed line respectively. The sum of the contributions of the lower- and higher-temperature components is shown as a solid line. Lower curves: plot of C_p against temperature for isolated abrin II A-subunit (92.8 μM) at pH 7.2 at a scan rate of 10 $K \cdot h^{-1}$. Resolution of the progress baseline-subtracted and concentration-normalized DSC data for abrin II A-subunit: ○, data points; solid line, two-state fit of the data.

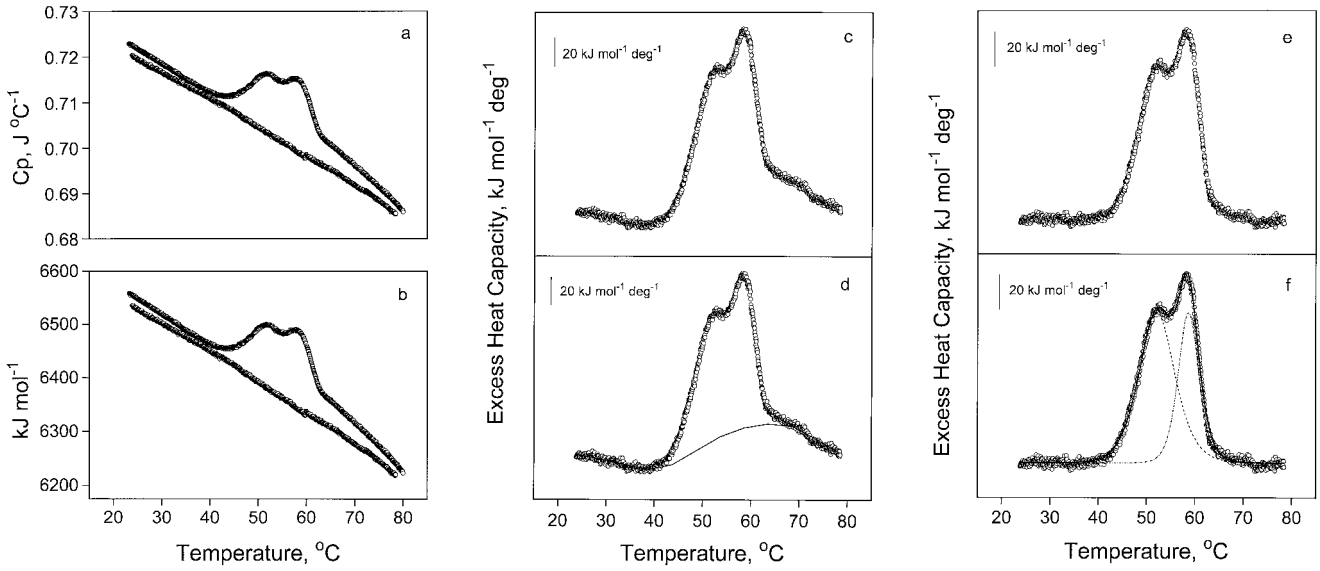

Figure 2 DSC scan of abrin II (92.8 μM) in the presence of 20 mM lactose, pH 7.2, at 10 K · h^{-1}

Graphic illustration of the baseline correction procedure used. (**a**) Upper curve: raw DSC data for calorimetric transition of abrin II in the presence of lactose compared with buffer alone. Lower curve: scan obtained with buffer in both sample and reference cells of the calorimeter. (**b**) Concentration-normalized (92.8 μM) raw data for the scans in (**a**). (**c**) Buffer/buffer baseline-subtracted raw data. (**d**) Progress baseline connection of pre- and post-transition baselines of the raw data shown in (**c**). (**e**) Progress baseline-subtracted DSC data used for fitting. (**f**) Final fitted calorimetric scan. The data points are shown as open circles (○). The two-state fits of the data to lower- and higher-temperature transitions are shown as a dashed line and as a dotted–dashed line respectively. The sum of the contributions of the lower- and higher-temperature components is shown as a solid line.

Table 1 Thermodynamic quantities for the thermal transition of abrin II and its isolated A-subunit as a function of pH

The DSC scan rate was 10 K · h^{-1}, except where indicated (*60 K · h^{-1}). T_{m1}, ΔH_{c1} and ΔH_{v1} are the respective values for the lower-temperature transition, while T_{m2}, ΔH_{c2} and ΔH_{v2} are the same quantities for the higher-temperature transition. The errors in the determination of T_m, ΔH_c and ΔH_v values were less than 0.05%, 3.0% and 3.5% respectively. The concentration of intact abrin II and of its isolated A-subunit was 92.8 μM.

pH	T_{m1} (K)	ΔH_{c1} (kJ · mol^{-1})	ΔH_{v1} (kJ · mol^{-1})	$\Delta H_{c1}/\Delta H_{v1}$	T_{m2} (K)	ΔH_{c2} (kJ · mol^{-1})	ΔH_{v2} (kJ · mol^{-1})	$\Delta H_{c2}/\Delta H_{v2}$
Abrin II								
4.50	340.8	1356	628	2.16	343.3	946	787	1.20
5.43	338.5	1230	611	2.01	340.1	854	749	1.14
5.80	334.4	1125	577	1.95	336.5	816	686	1.19
6.43	327.4	1067	552	1.93	331.1	766	615	1.24
6.83	324.2	937	452	2.07	328.4	686	594	1.15
7.20	319.2	854	410	2.08	324.6	573	515	1.11
7.82	317.2	736	381	1.93	323.8	527	494	1.07
8.30	314.8	586	301	1.94	321.0	519	469	1.11
9.16	311.6	561	276	2.03	318.2	452	464	0.97
10.16	309.8	456	234	1.95	316.4	410	414	0.99
7.20*	323.1	887	423	2.10	329.2	619	674	0.92
A-subunit								
4.50	–	–	–	–	322.9	494	502	0.98
7.20	–	–	–	–	322.2	506	519	0.98

854 kJ · mol^{-1}, while the higher-temperature transition peak has a T_m of 324.6 K with ΔH_m = 573 kJ · mol^{-1} (Table 1). If abrin II is scanned up to a temperature at which the lower-temperature transition peak mostly appears, and is then cooled and scanned again, then only the higher-temperature transition peak is observed, indicating that the lower-temperature transition peak is irreversible. If the sample is scanned yet again past the second transition, no endotherm appears, suggesting that the higher-temperature transition peak is also irreversible. To rule out any kinetic effects on the unfolding of abrin II, data were also collected at several scan rates (10–60 K · h^{-1}). There is a slight increase in the transition temperature with increase in scan rate, but the thermodynamic parameters, ΔH_c and ΔH_v, are independent of the scan rate. Therefore the two-state equilibrium model, and not the irreversible model [29], was applied to these transitions. The basis for this assumption is that the transition may be treated as a sequence of two processes; the first process is the reversible unfolding of the protein, described by thermodynamic parameters T_m, ΔH_v and ΔH_c, which is followed by a slower irreversible process, e.g. aggregation. This treatment,

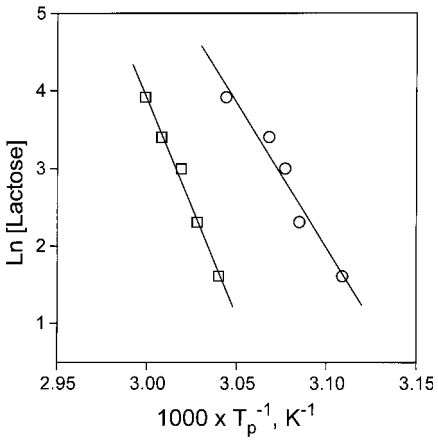

Figure 3 Plots of ln[lactose] against $1/T_p$ for abrin II

The lines are the best least-squares fits of ln[lactose] against $1/T_p$ for the lower- (○) and higher- (□) temperature transition peaks of abrin II (92.8 μM) in the presence of lactose at pH 7.2. The correlation coefficients are 0.96 and 0.99 for the lower- and higher-temperature transition peaks respectively. The scan rate was 10 K·h^{-1}.

first demonstrated by Sturtevant and co-workers [30], yields results for the overall process that are the same as for the reversible process. This less conservative view is supported by others [31,32] and justifies treating the unfolding transition of abrin II from the standpoint of a thermodynamic model.

A plot of C_p against temperature for the isolated A-subunit of abrin II is also shown in Figure 1 (lower curve). This transition, which is symmetrical, is characterized by a T_m of 322.2 K and a ΔH_c value of 506 kJ·mol^{-1}. These data are thus similar to those for the deconvoluted higher-temperature transition peak of abrin II. These data apparently indicate that, in intact abrin II, the higher-temperature transition peak at 324.6 K corresponds to its A-subunit. The values of ΔH_c for these transitions are comparable with those reported for other globular proteins [33]. A lower value (by 2.4 K) for the T_m of the isolated A-subunit than for the higher-temperature transition peak of intact abrin II implies some intersubunit interaction within the intact toxin which contributes to the increased stability of the A-subunit. The B-subunit becomes completely insoluble when separated from the A-subunit. Consequently, the thermal unfolding behaviour of the isolated B-subunit could not be characterized. It may be noted that the $\Delta H_c/\Delta H_v$ ratio for the low-temperature transition is nearly 2, while that for the high-temperature transition is close to 1. This indicates that, at their respective denaturation temperatures, two domains are involved in the unfolding of the first transition, while a single domain is implicated for the second one.

Stabilization by ligand binding

In the presence of saturating amounts of lactose, the values of T_m, ΔH_c and ΔH_v increased, indicating that lactose stabilizes the native conformation of abrin II (Figure 2). An increase in thermal stability due to an added ligand has been reported for a large number of proteins [34,35]. The denaturation transition for the liganded form can be written as follows [35]:

$$N_mL_n \leftrightarrow mD + nL \quad (5)$$

where m is the number of native (N) or denatured (D) protein molecules and n is the number of ligand (L) molecules. At constant protein concentration this can be transformed to:

$$\ln[L] = -\Delta H_v/(nRT_p) + \text{constant} \quad (6)$$

where T_p is the temperatue at which the transition peak is a maximum. The ΔH_v value (595 kJ·mol^{-1}) calculated from a plot of ln[lactose] against $1/T_p$ (with $n = 2$) for the lower-temperature transition is similar to the value obtained by the two-state fit of the transition data in the presence of lactose (Figure 3 and Table 2). Thus two lactose molecules bind to one molecule of abrin II. At equivalent concentrations of lactose, T_m for the first transition increases by 8.8 K at pH 7.2, while at pH 4.5 it increases by 5.5 K (Table 2). Although the second transition also shifts to higher temperatures in the presence of lactose, a strict correlation between ligand concentration and T_p is not discernible. A control experiment using isolated A-subunit saturated with 50 mM lactose gave identical results as with the A-subunit alone, indicating a lack of interaction of lactose with this subunit.

Effect of salt

The denaturation temperature of abrin II increases with increasing NaCl concentration, without an appreciable change in the co-operativity of the lower- and higher-temperature

Table 2 Thermodynamic quantities for the thermal transition of abrin II in the presence of lactose

The DSC scan rate was 10 K·h^{-1}. T_{m1}, T_{p1}, ΔH_{c1} and ΔH_{v1} are the respective values for the lower-temperature transition, while T_{m2}, ΔH_{c2}, T_{p2} and ΔH_{v2} are the same quantities for the higher-temperature transition. The errors in the determination of T_m, ΔH_c and ΔH_v values were less than 0.05%, 3.2% and 4.0% respectively. The concentration of abrin II was 92.8 μM.

Lactose (mM)	T_{p1} (K)	T_{m1} (K)	ΔH_{c1} (kJ·mol^{-1})	ΔH_{v1} (kJ·mol^{-1})	$\Delta H_{c1}/\Delta H_{v1}$	T_{p2} (K)	T_{m2} (K)	ΔH_{c2} (kJ·mol^{-1})	ΔH_{v2} (kJ·mol^{-1})	$\Delta H_{c2}/\Delta H_{v2}$
pH 7.2										
0	–	319.2	854	410	2.08	–	324.6	573	515	1.11
5*	321.5	321.8	904	481	1.88	328.9	328.7	590	523	1.13
10	324.0	323.6	954	473	2.02	330.2	330.2	540	536	1.01
20	324.9	324.7	987	540	1.83	331.1	331.5	565	548	1.03
30	325.9	325.6	1008	586	1.72	332.3	332.5	561	540	1.04
50	328.4	328.0	1117	602	1.85	333.2	333.9	577	556	1.04
pH 4.5										
0	–	340.8	1180	623	1.89	–	343.3	787	778	1.01
50	–	346.3	1209	623	1.94	–	348.3	828	883	0.94

* The ratio $K_{b(DSC)}/K_{b(ITC)}$ (471/508) i.e., the binding constant at the denaturation temperature determined by DSC to the extrapolated value of binding constant determined by ITC is 0.93

Table 3 Thermodynamic quantities for the thermal transition of abrin II in the presence of NaCl

The DSC scan rate was 10 K·h^{-1}. T_{m1}, ΔH_{c1} and ΔH_{v1} are the respective values for the lower-temperature transition, while T_{m2}, ΔH_{c2} and ΔH_{v2} are the same quantities for the higher-temperature transition. The errors in the determination of T_m, ΔH_c and ΔH_v values were less than 0.05%, 2.7% and 3.0% respectively. The concentration of abrin II was 92.8 μM.

NaCl (mM)	T_{m1} (K)	ΔH_{c1} (kJ·mol^{-1})	ΔH_{v1} (kJ·mol^{-1})	$\Delta H_{c1}/\Delta H_{v1}$	T_{m2} (K)	ΔH_{c2} (kJ·mol^{-1})	ΔH_{v2} (kJ·mol^{-1})	$\Delta H_{c2}/\Delta H_{v2}$
150	321.5	895	485	1.84	326.7	598	540	1.11
500	322.3	937	506	1.85	329.0	632	569	1.11
1000	325.2	925	519	1.78	331.8	686	661	1.04

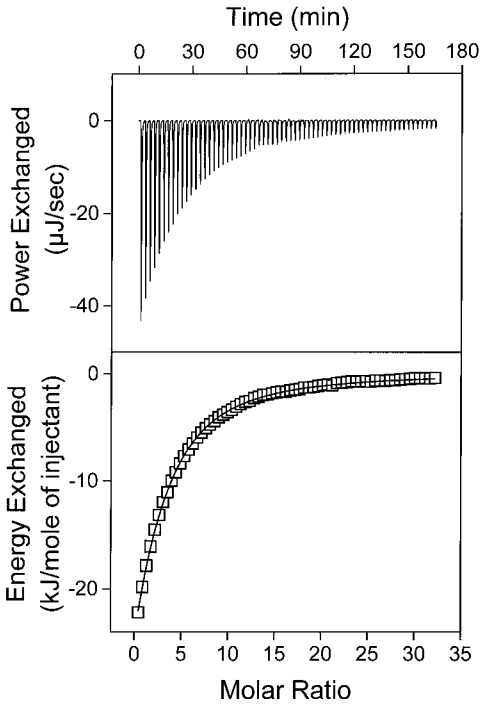

Figure 4 Calorimetric titration of abrin II with lactose

Upper panel: raw data obtained for 66 automatic injections, each of 5 μl of 10.5 mM lactose into 351 μM abrin II solution at 282.1 K. Lower panel: total heat released as a function of the molar ratio of lactose to abrin II for the titration shown in the upper panel. The solid line is the result of the least-squares fit of the data to eqn. (3). The buffer used was 50 mM sodium phosphate, pH 7.2.

transitions. This implies increased stability of the protein with increasing salt concentration (Table 3).

Binding of lactose to abrin II

A typical isothermal measurement of the binding of lactose to abrin II, along with a least-squares fit of the data to the identical-site model, is given in Figure 4. The fit of the data to the identical-site model shows that two lactose molecules bind to one molecule of abrin II, with values for K_b (the binding constant) and ΔH_b (the binding enthalpy) of 2980 ± 56 M^{-1} and 33472 ± 408 kJ·mol^{-1} respectively. The binding constant at denaturation temp, $K_b(T_c)$, calculated using eqn. (2), is in good agreement with the value obtained from ITC measurements, which is extrapolated to the denaturation temperature (Table 2).

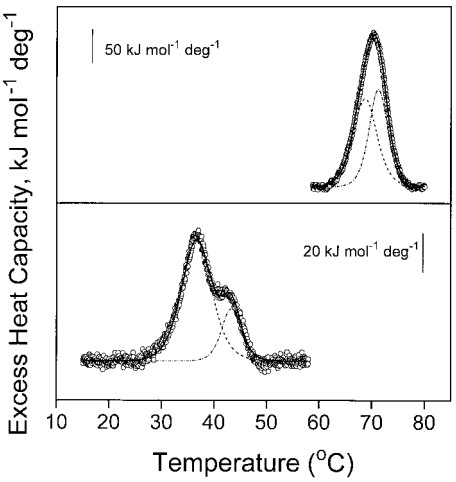

Figure 5 DSC scans of 92.8 μM abrin II at pH 4.50 and at pH 10.16

Resolution of the progress baseline-subtracted and concentration-normalized DSC data for abrin II at pH 4.5 (upper panel) and pH 10.16 (lower panel) into two independent two-state curves. The data points are shown as open circles (○). The two-state fits of the data to lower- and higher-temperature transitions are shown as a dashed line and as a dotted–dashed line respectively. The sum of the contributions of the lower- and higher-temperature components is shown as a solid line. The scan rate was 10 K·h^{-1}; the buffers used were 50 mM sodium acetate (pH 4.50) and 50 mM sodium carbonate (pH 10.16).

Effect of pH

Calorimetric scans were also carried out as a function of pH in the pH range 4.5–10.2. The results of the fits of the data are given in Table 1. DSC scans at the two pH extremes, i.e. pH 4.5 and 10.2, are shown in Figure 5. A plot of ΔH_c against T_m is shown in Figure 6. The data are fitted to a straight line using linear regression analysis (Origin program). The slope ($d\Delta H_c/dT_m$) gives the estimate of ΔC_p. The values of ΔC_p obtained from Figure 6 are 27 ± 2 kJ·mol^{-1}·K^{-1} and 20 ± 1 kJ·mol^{-1}·K^{-1} for the lower- and higher-temperature transition peaks respectively.

The free energy changes for these transitions as a function of temperature, $\Delta G°(T)$, are calculated from the values of T_m, ΔH_m and ΔC_p using the Gibbs–Helmholtz equation:

$$\Delta G°(T) = \Delta H_m[(T_m - T)/T_m] + \Delta C_p[T - T_m - T\ln(T/T_m)] \quad (7)$$

The values of ΔH_m, T_m and ΔC_p used for the low-temperature transition at pH 7.2 are 854 kJ·mol^{-1}, 319.2 K and 27 kJ·mol^{-1}·K^{-1} respectively. For the higher-temperature transition at pH 7.2, they are $\Delta H_m = 573$ kJ·mol^{-1}, $T_m = 324.6$ K and $\Delta C_p = 20$ kJ·mol^{-1}·K^{-1}.

The temperature at which the lower-temperature transition (B-subunit) of abrin II is maximally stable is 289 ± 2 K, with a free energy of stabilization of 41 ± 3 kJ·mol^{-1}. For the higher-temper-

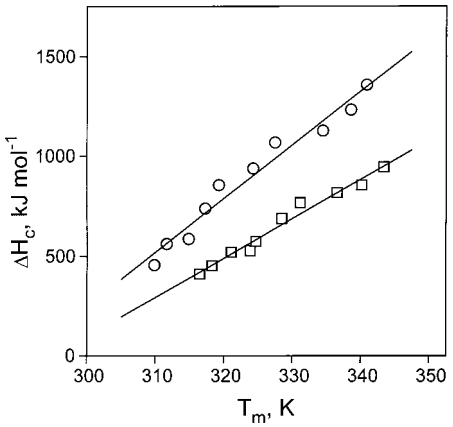

Figure 6 Plots of ΔH_m against T_m for 92.8 μM abrin II

The solid lines are least-squares fits for the lower- (○) and higher- (□) temperature transition peaks. The correlation coefficients are 0.97 and 0.98 for the lower- and higher-temperature transition peaks respectively. The slopes of these lines yield ΔC_p values of 27 ± 2 kJ·mol^{-1}·K^{-1} and 20 ± 1 kJ·mol^{-1}·K^{-1} for the lower- and higher-temperature transition peaks respectively.

ature transition (A-subunit), the maximum stabilization temperature is 297 ± 2 K, with a free energy of stabilization of 25 ± 1 kJ·mol^{-1}. Cold denaturation temperatures are predicted to be 270 ± 3 K and 260 ± 4 K respectively for the higher- and lower-temperature transition peaks. The thermal stability of intact abrin II increases at pH 4.5. However, no such effect was observed for the isolated A-subunit (Table 1).

DISCUSSION

Abrin II is a heterodimeric protein consisting of A- and B-subunits connected by a single disulphide bond. The DSC scan of abrin II shows two peaks, indicating that the protein consists of two entities unfolding at different temperatures. The values of T_m and ΔH_c for the higher-temperature transition peak are similar to those for the isolated A-subunit. Hence the higher-temperature transition is identified with the unfolding of the A-subunit at the denaturation temperature. The lower-temperature transition exhibits a value of 2 for the $\Delta H_c/\Delta H_v$ ratio, suggesting that it represents the unfolding of two domains at the denaturation temperature. The data also indicate that these domains display identical thermal unfolding properties. Moreover, these domains appear to unfold, to a large extent, completely independently under a variety of conditions employed in these studies. These results also imply that the unfolding of the first transition is less co-operative than would be expected if the two domains were interacting with each other to a significant extent. This is not surprising if one examines the three-dimensional structure of abrin II. In the abrin a (abrin II of these studies) structure, the two carbohydrate-binding domains of the B-subunit appear to interact very little with each other. The B-subunit is insoluble in aqueous solution when separated from the A-subunit. This could be due to the B-subunit being more hydrophobic, a view consistent with the higher value of ΔC_p associated with its thermal unfolding [36]. Unlike the other isoforms of abrin, we were unable to solubilize the B-subunit with ionic and non-ionic detergents or by carboxymethylation of its thiol groups either with or without detergents [37]. These results indicate that the toxin is mostly stabilized by intrasubunit interactions, with very little intersubunit interaction, unlike DT, which is stabilized by a combination of intra- and inter-subunit interactions.

In the absence of similar studies on other RIPs, it is instructive to compare the thermal unfolding behaviour of DT and cholera toxin with that of abrin II. Intact DT, like abrin II, displays two thermal unfolding transitions [14]. The denaturation temperature of the isolated A-subunit of DT is 6.5 K lower than that of the lower-temperature transition (A-subunit) of intact DT. The B-subunit of DT is hydrophobic and is precipitated when separated from the A-subunit. Thus the thermal unfolding behaviours of DT and abrin II appear quite similar. In contrast, the A- and B-subunits of cholera toxin unfold independently. This observation was confirmed by the fact that the T_m and ΔH_c values of isolated B-subunits were similar to those of the higher-temperature transition peak (B-subunit) of cholera toxin [38]. Similar observations have also been made in the case of several multidomain proteins, which are stabilized by intradomain interactions and not by interdomain interactions [39].

The T_m and ΔH_c values of abrin II increase with decreases in pH, while the stability of the isolated A-subunit remains unchanged at various pH values (Table 1). There is an upward shift of approx. 22 K in the T_m between pH 7.2 and pH 4.5. Thus the stability of intact abrin II increases as the pH is lowered from neutral to pH 4.5. The stabilization at pH 4.5 could be due to a potentiation of interactions between the A- and B-subunits. Similar results are also observed for the guanidine hydrochloride-induced unfolding of abrin II and its A-subunit (J. Krupakar, P. K. Das and S. K. Podder, unpublished work). Unfolding experiments using guanidine hydrochloride show that the stabilities of ricin and mistletoe lectin and their A-subunits are greater at lower pH values [17,18]. The ΔC_p values observed in the case of abrin II, especially for its B-subunit, are higher than those for small globular proteins, and are consistent with the high proportion of hydrophobic residues in RIPs [36]. This is in turn consistent with the ability of these proteins to penetrate membranes [15,16].

The binding of lactose stabilizes the entire toxin, as indicated by the increased values of T_m and ΔH_m for both transitions, suggesting that there is an interaction between the two subunits of the RIP. At equivalent concentrations of lactose and abrin II, the T_m shifts by approx. 8 K at pH 7.2 and approx. 4 K at pH 4.5, indicating that the ligand-induced stabilization is more pronounced at pH 7.2 than at pH 4.5. In the case of ricin, the values for the binding constant and binding stoichiometry with galactose at low pH are 10 and 25% respectively of those observed at neutral pH [40]. The lesser shift of T_m (by 4 K) in the case of abrin II ligated with lactose at pH 4.5 could be due either to weak binding of lactose to the native abrin II and/or to a decrease in the number of binding sites at acidic pH. The binding of two lactose molecules to one molecule of abrin II was surmised from the plot of ln[lactose] against $1/T_p$ for the lower-temperature transition. Similar results were obtained from ITC measurements. Furthermore, $K_{b(DSC)}/K_{b(ITC)}$ is close to 1, implying that lactose interacts with the folded form of abrin II preferentially. As the $\Delta H_c/\Delta H_v$ ratio remains the same for the ligated form, it is apparent that the ligand stabilizes both domains to the same extent, and that one molecule of the carbohydrate ligand binds to each of these domains. This is consistent with the crystal structure of abrin-a, whose B-subunit consists of two similar subdomains and each subdomain contains one carbohydrate-binding site; this is presumed to have occurred by gene duplication [41]. Two binding sites have also been observed in the other isoforms of abrin [42,43].

Although the increase in thermal stability and poor binding to lactose at low pH appear contradictory and not conducive to the

release of the toxin into the cytosol, these data provide us with additional insight into the mechanism of transmembrane translocation of the toxic A-subunit of type II RIPs. The low pH in the endosomal compartment would allow dissociation of a significant proportion of the toxin from its receptor, thus facilitating recycling of the latter to the cell surface. The higher stability of the free toxin in the lumen of the endosome not only would enable it to resist degradation, but also would permit it to make its way to the Golgi apparatus and endoplasmic reticulum. On reaching the endoplasmic reticulum, the high pH of this compartment would destabilize the toxin, thus permitting reduction of the intersubunit disulphide bond and insertion of the highly hydrophobic B-subunit into the membrane. The A-subunit would then be able to enter the cytosol through the channel formed by the B-subunits or via retrotranslocation [44].

This work was supported by the Department of Science and Technology and the Council of Scientific and Industrial Research, India. S.K.P. is a CSIR Emeritus Scientist.

REFERENCES

1 Olsnes, S. and Phil, A. (1982) in Molecular Action of Toxins and Viruses (Cohen, P. and van Heyningen, S., eds.), pp. 51–105, Elsevier, New York
2 Endo, Y., Mitsui, K., Motizuki, M. and Tsurugi, K. (1987) J. Biol. Chem. **262**, 5908–5912
3 Sandvig, K., Olsnes, S. and Phil, A. (1976) J. Biol. Chem. **251**, 3977–3984
4 Youle, R. J. and Neville, Jr., D. M. (1982) J. Biol. Chem. **257**, 1598–1601
5 Thorpe, P. E., Blakey, D. C., Brown, A. N. F., Knowles, P. P., Knyba, R. E., Wallace, P. M., Watson, G. J. and Wawtzynczak, E. J. (1987) J. Natl. Cancer Inst. **79**, 1101–1111
6 Refsnes, K., Olsnes, S. and Pihl, A. (1974) J. Biol. Chem. **249**, 3557–3562
7 Montesano, D., Cawley, D. and Herschman, H. R. (1982) Biochem. Biophys. Res. Commun. **109**, 7–13
8 Beaumelle, B., Alami, M. and Hopkins, C. R. (1993) J. Biol. Chem. **268**, 23661–23669
9 Yoshida, T., Chen, C., Zhang, M. and Wu, H. C. (1991) Exp. Cell Res. **192**, 389–395
10 Simpson, J. C., Dascher, C., Roberts, L. M., Lord, J. M. and Balch, W. E. (1995) J. Biol. Chem. **270**, 20078–20083
11 Rapak, A., Falnes, P.Ø. and Olsnes, S. (1997) Proc. Natl. Acad. Sci. U.S.A. **94**, 3783–3788

Received 8 June 1998/27 October 1998; accepted 2 December 1998

12 Beaumelle, B., Bensammar, L. and Bienvenue, A. (1992) J. Biol. Chem. **267**, 11525–11531
13 London, E. (1992) Biochim. Biophys. Acta **1113**, 25–51
14 Ramsay, G., Montgomery, D., Berger, D. and Freire, E. (1989) Biochemistry, **28**, 529–533
15 Ishida, B., Cawley, D. B., Reue, K. and Wisnieski, B. J. (1983) J. Biol. Chem. **258**, 5933–5937
16 Ramalingam, T. S., Das, P. K. and Podder, S. K. (1994) Biochemistry **33**, 12247–12254
17 Bushueva, T. L. and Tonevitsky, A. G. (1987) FEBS Lett. **215**, 155–159
18 Bushueva, T. L., Tonevitsky, A. G., Kindt, A. and Franz, H. (1988) Mol. Biol. (Moscow) **22**, 628–634
19 Hegde, R., Maiti, T. K. and Podder, S. K. (1991) Anal. Biochem. **194**, 101–109
20 Olsnes, S. (1978) Methods Enzymol. **50**, 322–330
21 Schellman, J. A. (1975) Biopolymer **14**, 999–1018
22 Schwarz, F. P., Puri, K. and Surolia, A. (1991) J. Biol. Chem. **266**, 24344–24350
23 Wiseman, T., Williston, S., Brandts, J. F. and Lin, L. N. (1989) Anal. Biochem. **179**, 131–137
24 Yang, C. P. (1990) Omega Data in Origin, p. 66, Microcal Inc., Northampton, MA
25 Ladury, J. E., Kishore, N., Hellinga, H. W., Wynn, R. and Sturtevant, J. M. (1994) Biochemistry **33**, 3688–3692
26 Ganesh, C., Shah, A. N., Swaminathan, C. P., Surolia, A. and Varadarajan, R. (1997) Biochemistry **36**, 5020–5028
27 Privalov, P. L. and Khechinashvili, N. N. (1974) J. Mol. Biol. **86**, 665–684
28 Robertson, A. D. and Murphy, K. P. (1997) Chem. Rev. **97**, 1251–1267
29 Sanchez-Ruiz, J. M., Lopez-Lacomba, J. L., Cortijo, M. and Mateo, P. L. (1988) Biochemistry **27**, 1648–1652
30 Manly, S. P., Mattews, K. S. and Sturtevant, J. M. (1985) Biochemistry **24**, 3842–3846
31 Ross, P. D. and Shrake, A. (1988) J. Biol. Chem. **263**, 11196–11202
32 Brandts, J. F., Hu, C. Q., Lin, L. and Mas, M. T. (1989) Biochemistry **28**, 8588–8596
33 Privalov, P. L. (1982) Adv. Protein Chem. **35**, 1–104
34 Surolia, A., Sharon, N. and Schwarz, F. P. (1996) J. Biol. Chem. **271**, 17697–17703
35 Fudaka, H., Sturtevant, J. M. and Quiocho, F. A. (1983) J. Biol. Chem. **258**, 13193–13198
36 Privalov, P. L. (1979) Adv. Protein Chem. **33**, 167–241
37 Chen, J.-K., Hung, C.-H., Liaw, Y.-C. and Lin, J.-Y. (1997) Protein Eng. **10**, 827–833
38 Goins, B. and Freire, E. (1988) Biochemistry **27**, 2046–2052
39 Pabo, C. O., Sauer, R. T., Sturtevant, J. M. and Ptashne, M. (1979) Proc. Natl. Acad. Sci. U.S.A. **76**, 1608–1612
40 Frenoy, J.-P. (1986) Biochem. J. **240**, 221–226
41 Tahirov, T. H., Lu, T.-H., Liaw, Y.-C., Chen, Y.-L. and Lin, J.-Y. (1995) J. Mol. Biol. **250**, 354–367
42 Ohba, H., Yamasaki, N. and Funatsu, G. (1990) Agric. Biol. Chem. **54**, 1995–2001
43 Ohba, H., Yamasaki, N., Eguchi, K. and Funatsu, G. (1993) Biosci. Biotechnol. Biochem. **57**, 1409–1413
44 Hazes, B. and Read, R. J. (1997) Biochemistry **36**, 11051–11054